

# Dark matter properties and axion dark radiation from rotation curves and energy cascade

Zhijie (Jay) Xu,<sup>1\*</sup>

<sup>1</sup>Physical and Computational Sciences Directorate, Pacific Northwest National Laboratory; Richland, WA 99354, USA

Accepted XXX. Received YYY; in original form ZZZ

## ABSTRACT

We present a cascade theory to predict dark matter (DM) particle mass, size, lifetime, and properties of possible dark radiation from DM decay. The existence of inverse mass and energy cascade from small to large scales facilitates the hierarchical structure formation in dark matter flow. A scale-independent constant rate of energy cascade  $\varepsilon_u \approx -4.6 \times 10^{-7} m^2/s^3$  can be identified. The energy cascade leads to a two-thirds law for pairwise velocity and a four-thirds law for halo density. Both scaling laws can be directly confirmed by N-body simulations and galaxy rotation curves. For collisionless dark matter with only gravity involved, scaling laws can be extended down to the smallest scale, where quantum effects become important. Combining  $\varepsilon_u$ , Planck constant  $\hbar$ , and gravitational constant  $G$  on that scale, we predict DM particles have a mass  $m_X = (\varepsilon_u \hbar^5 G^{-4})^{1/9} = 0.9 \times 10^{12} \text{GeV}$ , a size  $l_X = (\varepsilon_u^{-1} \hbar G)^{1/3} = 3 \times 10^{-13} \text{m}$ , and a lifetime  $\tau_X = c^2/\varepsilon_u = 10^{16} \text{yrs}$ , where  $c$  is the speed of light. The energy scale  $E_X = (\varepsilon_u^5 \hbar^7 G^{-2})^{1/9} = 10^{-9} \text{eV}$  strongly suggests a dark "radiation" field to provide a viable mechanism for energy dissipation. If existing, the dark "radiation" should be produced at an early time  $t_X = (\varepsilon_u^{-5} \hbar^2 G^2)^{1/9} = 10^{-6} \text{s}$  (quark epoch) with a particle mass of  $10^{-9} \text{eV}$  such that axion can be a very promising candidate. If axion is the dark "radiation", it should have a mass of  $E_X$  ( $10^{-9} \text{eV}$ ) with a GUT scale decay constant  $10^{16} \text{GeV}$  and an effective axion-photon coupling constant  $10^{-18} \text{GeV}^{-1}$ . The energy density of dark radiation is about  $\Omega_a h^2 \approx 2.6 \times 10^{-7}$ , i.e. 1% of the photon energy in CMB or an equivalent increase in the effective number of neutrino  $\Delta N_{eff} = 0.02$ . Potential extension to self-interacting dark matter is also presented. Since the DM particle mass  $m_X$  is only weakly dependent on  $\varepsilon_u$  as  $m_X \propto \varepsilon_u^{1/9}$ , the estimation of  $m_X$  should be pretty robust for a wide range of possible values of  $\varepsilon_u$ . If gravity is the only interaction and dark matter is fully collisionless, mass of  $10^{12} \text{GeV}$  seems required to produce the given rate of energy cascade  $\varepsilon_u$ . In other words, if DM particle mass has a different value, there must be some new interaction beyond gravity. This work suggests a heavy dark matter scenario with a mass much greater than WIMPs.

**Key words:** Dark matter; Dark radiation; N-body simulations; Rotation curve; Collisionless; Self-interacting;

## CONTENTS

- 1 Introduction
- 2 Constant rate of energy cascade
- 3 Two-thirds law from simulation
- 4 Five-thirds and Four-thirds laws
- 5 Collisionless dark matter properties
- 6 Axion dark "radiation" and its properties
- 7 Self-interacting dark matter
- 8 Conclusions

## 1 INTRODUCTION

The existence of dark matter (DM) is supported by numerous astronomical observations. The most striking indications come from the dynamical motions of astronomical objects. The flat rotation curves of spiral galaxies point to the existence of galactic dark matter haloes with a total mass much greater than luminous matter (Rubin & Ford

1970; Rubin et al. 1980). The Planck measurements of the cosmic microwave background (CMB) anisotropies concludes that the amount of dark matter is about 5.3 times that of baryonic matter based on the standard  $\Lambda$ CDM cosmology (Aghanim et al. 2021).

In the standard CDM paradigm of cosmology, dark matter is cold (non-relativistic), collisionless, dissipationless, non-baryonic, and barely interacting with baryonic matter except through gravity (Peebles 1984; Spergel et al. 2003; Komatsu et al. 2011; Frenk & White 2012). Despite its great successes in the formation and evolution of large scale structures, theoretical and observational difficulties also exist (Perivolaropoulos & Skara 2022; Bullock & Boylan-Kolchin 2017). Cold dark matter predictions on small scales are inconsistent with some observations. This is generally known as the core-cusp problem (Flores & Primack 1994; de Blok 2010), the missing satellite problem (Klypin et al. 1999; Moore et al. 1999), and the too-big-to-fail problem (Boylan-Kolchin et al. 2011, 2012). To solve these problems, both non-cold and non-collisionless dark matter models were also proposed as natural solutions. Examples are the warm dark matter (WDM) with a steep suppression of the power spectrum at small scales (Viel et al. 2013) and the self-interacting dark matter (SIDM) (Spergel & Steinhardt 2000; Tulin & Yu 2018).

\* E-mail: zhijie.xu@pnnl.gov; zhijie.xu@hotmail.com

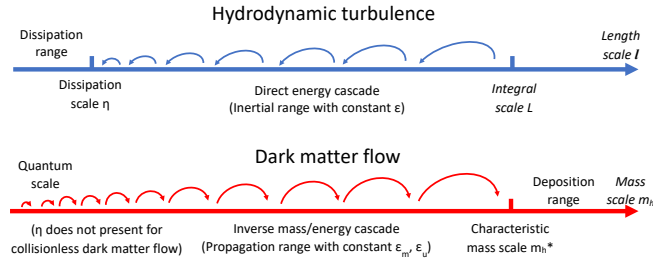


**Figure 1.** Schematic plot of the direct energy cascade in turbulence and the inverse mass and energy cascade in dark matter flow. Haloes merge with single mergers to facilitate a continuous mass and energy cascade to large scales. Scale-independent mass flux  $\varepsilon_m$  and energy flux  $\varepsilon_u$  are expected for haloes smaller than a characteristic mass scale (i.e. the propagation range corresponding to the inertial range for turbulence). Mass cascaded from small scales is consumed to grow haloes at scales above the characteristic mass  $m_h^*$  (the deposition range similar to the dissipation range in turbulence), where mass and energy flux become scale-dependent.

Though the nature of dark matter is still unclear, it is often assumed to be a thermal relic, weakly interacting massive particles (WIMPs) that were in local equilibrium in the early universe (Steigman & Turner 1985). These thermal relics freeze out as the reaction rate becomes comparable with the expansion of universe. The self-annihilation cross section required by the right DM abundance is on the same order as the typical electroweak cross section, in alignment with the supersymmetric extensions of the standard model ("WIMP miracle") (Jungman et al. 1996). The mass of thermal WIMPs ranges from a few GeV to hundreds GeV with the unitarity argument giving an upper bound of several hundred TeV (Griest & Kamionkowski 1990). However, no conclusive signals have been detected in either direct or indirect searches for thermal WIMPs in that range of mass. This might hint a different thinking required beyond the standard WIMP paradigm. The other strongly motivated dark matter candidate can be the axion from the Peccei–Quinn (PQ) solution to the strong CP problem. Axions satisfy the two conditions of cold dark matter: a sufficient non-relativistic amount that provide the required matter density and the effectively collisionless nature (Duffy & van Bibber 2009). In addition, relativistic axion can also be a promising candidate of dark radiation due to its small mass and weak interaction with standard model particles (Mazumdar et al. 2016; Marsh 2016).

In this paper, we primarily focus on the cold particle dark matter that is sufficiently smooth on large scales with a fluid-like behavior best described by a self-gravitating collisionless fluid dynamics (SG-CFD). A complete understanding of the nature of dark matter flow may provide key insights into the properties of dark matter particles. This paper introduces a new perspective that is based on the scaling laws established for the flow of dark matter, which can be confirmed by both galaxy rotation curves and N-body simulations. Dark matter particle properties might be inferred by consistently extending established scaling laws down to the smallest scale (Section 5), beyond which quantum effects become dominant. On that scale, the dark radiation is naturally required to provide a viable mechanism for energy dissipation. Properties and abundance of dark radiation can also be inferred to help direct/indirect detection (Section 6).

At first glimpse, both SG-CFD and hydrodynamic turbulence contain the same essential ingredients, i.e. randomness, nonlinearity, and multiscale nature. This suggests a quick revisit of some fundamental ideas of turbulence, a long-standing unresolved problem in classical physics. Turbulence is ubiquitous in nature. In particular, homogeneous isotropic incompressible turbulence has been well-studied for

many decades (Taylor 1935, 1938; de Karman & Howarth 1938; Batchelor 1953). Turbulence consists of a random collection of eddies (building blocks of turbulence) on different length scales that are interacting with each other and dynamically changing in space and time. The classical picture of turbulence is an eddy-mediated cascade process, where kinetic energy of large eddies feeds smaller eddies, which feeds even smaller eddies, and so on to the smallest scale  $\eta$  where viscous dissipation is dominant (see Fig. 1). The direct energy cascade can be described by a poem (Richardson 1922):

"Big whirls have little whirls, That feed on their velocity;  
And little whirls have lesser whirls, And so on to viscosity."

Provided the Reynolds number is high enough, there exists a range of length scales where the viscous force is negligible and the inertial force is dominant (inertial range). The rate  $\varepsilon$  (unit:  $m^2/s^3$ ) of energy passing down the cascade is scale-independent in the inertial range and only related to eddy velocity  $u$  and size  $l$  as  $\varepsilon \propto u^3/l$ . This rate matches exactly the rate of energy dissipation due to viscosity  $\nu$  on the smallest scale  $\eta$  (Fig. 1). The inertial range extends down to the smallest (Kolmogorov) scale  $\eta = (\nu^3/\varepsilon)^{1/4}$ , below which is the dissipation range (Fig. 1). While direct energy cascade exists in 3D turbulence, there exists an inverse energy cascade in 2D turbulence with energy transferred from small to large scales (Kraichnan 1967), which is similar to the flow of dark matter in Fig. 1.

For inertial range of incompressible turbulence with a constant energy flux  $\varepsilon$ , a universal scaling is established for the  $m$ th order longitudinal velocity structure function (Kolmogorov 1962) (or  $m$ th moments of the pairwise velocity in cosmology terms),

$$S_m^{lp}(r) = \left\langle (u'_L - u_L)^m \right\rangle = \beta_m \varepsilon^{m/3} r^{m/3} \quad (1)$$

and for second order moment with  $m=2$ ,

$$S_2^{lp}(r) = \beta_2 \varepsilon^{2/3} r^{2/3} \quad \text{or} \quad \varepsilon = \frac{(S_2^{lp}/\beta_2)^{3/2}}{r} = \frac{u^2}{r/u} = \frac{u^3}{r}. \quad (2)$$

The constant  $\beta_2 \approx 2$  for  $m=2$ , where  $u'_L$  and  $u_L$  are two longitudinal (or pairwise) velocities (see Fig. 3 for definition). Here  $r$  is the scale of separation or eddy size and  $u$  is eddy's characteristic speed. Equation (2) describes the cascade of kinetic energy  $u^2$  to smaller eddies within a typical eddy turnaround time  $r/u$ .

Now go back to the flow of dark matter that exhibits different behaviors due to its collisionless and long-range interaction nature. Does this simple scaling law (Eqs. (1) and (2)) also apply to dark matter properties? If yes, how does it enhance our understanding of dark matter properties? These are the critical questions we will try to answer in this paper.

First, we note that highly localized haloes are a major manifestation of nonlinear gravitational collapse (Neyman & Scott 1952; Cooray & Sheth 2002). As the building blocks of SG-CFD (counterpart to "eddies" in turbulence), haloes facilitate an inverse mass cascade that is absent in hydrodynamic turbulence (Fig. 1). The halo-mediated inverse mass cascade is fully consistent with the hierarchical structure formation, where haloes grow by a series of sequential merging along the chain of merging in Fig. 2. As shown in Fig. 2, haloes pass their mass onto larger and larger haloes, until halo mass growth becomes dominant over mass propagation. Consequently, there is a continuous cascade of mass from smaller to larger mass scales with a mass flux  $\varepsilon_m$  independent of the mass scale in a certain range (propagation range in Fig. 1). For halo group of all haloes with the same mass in that range, the mass flux into that group balances the mass flux out of the same group such that the total mass of that group does not vary with time. These halo groups simply propagates mass to large scales. Mass cascaded from small scales is eventually consumed

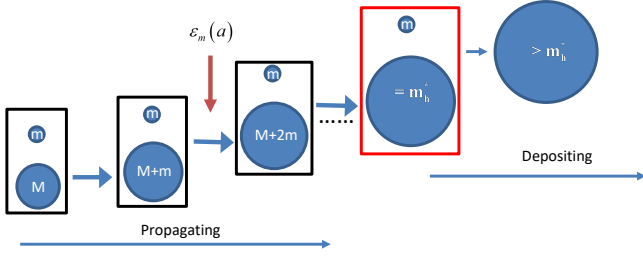


**Figure 2.** Schematic plot of the inverse mass cascade for hierarchical structure formation. Haloes of mass  $M$  merge with single merger (free DM particles of mass  $m$ ) to cause the mass flux into haloes on a larger scale  $M + m$  and the next merging along the chain. This facilitates a continuous mass cascade from small to large scales. A scale-independent mass flux  $\varepsilon_m$  is expected for haloes in the mass propagation range ( $< m_h^*$ ). Mass cascaded from small scales is finally consumed to grow halo mass at scales  $> m_h^*$ .

to grow halo mass in the deposition range at scales  $> m_h^*$ . From this description, the mass cascade can be described similarly with "eddies" (or "whirls") simply replaced by "haloes":

"Little haloes have big haloes, That feed on their mass;  
And big haloes have greater haloes, And so on to growth."

Second, haloes have certain kinetic and potential energy. Therefore, accompanied by the mass cascade, there also exists an energy flux (energy cascade) across haloes on different scales. The kinetic energy is also cascaded from small to large scales (same as mass cascade), while potential energy is cascaded in the opposite direction. Both turbulence and dark matter flow are non-equilibrium systems that can never reach a final equilibrium. Both types of flow involve an constant energy cascade rate  $\varepsilon_u$  in propagation range. The mass/energy cascade is an intermediate statistically steady state for non-equilibrium systems to continuously maximize system entropy while evolving towards the limiting equilibrium. Both SG-CFD and 2D turbulence exhibit an inverse (kinetic) energy cascade, while 3D turbulence possesses a direct energy cascade (Fig. 1).

Finally, while viscous dissipation is the only mechanism to dissipate the kinetic energy in turbulence, it is not present in collisionless dark matter flow. Without a viscous force, there is no dissipation range in SG-CFD and the smallest length scale of inertial range is not limited by viscosity. If there are no other known interactions or forces involved except gravity, this unique feature enables us to extend the scale-independent constant  $\varepsilon_u$  down to the smallest scale, where quantum effects become important. In addition, kinetic energy in collisionless dark matter flow continuously increase with time due to the gravitational collapse. The linear increase of system kinetic energy with time can be used to estimate the constant rate of cascade  $\varepsilon_u$  (see Eq. (4)). In this paper, we will present relevant scaling laws and apply them for dark matter and dark radiation properties.

## 2 CONSTANT RATE OF ENERGY CASCADE

The basic dynamics of dark matter flow follows from the collisionless Boltzmann equations (CBE) (Mo et al. 2010). Alternatively, particle-based gravitational N-body simulations are widely used to study the dynamics of dark matter flow (Peebles 1980). The simulation data for this work was generated from N-body simulations carried out by the Virgo consortium. A comprehensive description of this simulation can be found in (Frenk et al. 2000; Jenkins et al. 1998). This set of simulations has been widely used in studies such as clustering

statistics (Jenkins et al. 1998), the formation of halo clusters in large scale environments (Colberg et al. 1999), and testing models for halo abundance and mass functions (Sheth et al. 2001). More recent large scale cosmological  $\Lambda$ CDM simulations Illustris (Illustris-1-Dark) were also used in this work to validate the predicted scaling laws in Section 4 (Nelson et al. 2015).

When a self-gravitating system in expanding background is concerned, the evolution of system energy can be described by a cosmic energy equation (Irvine 1961; Layzer 1963),

$$\frac{\partial E_y}{\partial t} + H(2K_p + P_y) = 0, \quad (3)$$

which describes the energy conservation in expanding background. Here  $K_p$  is the specific (peculiar) kinetic energy,  $P_y$  is the specific potential energy in physical coordinate,  $E_y = K_p + P_y$  is the total energy,  $H = \dot{a}/a$  is the Hubble parameter, and  $a$  is the scale factor.

The cosmic energy equation (3) admits a linear solution of  $K_p = -\varepsilon_u t$  and  $P_y = (4/3)\varepsilon_u t$  for radiation dominated era with  $Ht = 1/2$ . While for matter dominated era with  $Ht = 2/3$ , the solutions becomes  $K_p = -\varepsilon_u t$  and  $P_y = (7/5)\varepsilon_u t$ . A constant rate of kinetic energy cascade ( $\varepsilon_u < 0$  for inverse cascade) can be defined as

$$\varepsilon_u = -\frac{K_p}{t} = -\frac{3}{2} \frac{u^2}{t} = -\frac{3}{2} \frac{u_0^2}{t_0^3} \approx -4.6 \times 10^{-7} \frac{m^2}{s^3}, \quad (4)$$

where  $u_0 \equiv u(t=t_0) \approx 354.6 \text{ km/s}$  is the one-dimensional velocity dispersion of dark matter particles from Virgo simulation, and  $t_0 \approx 13.7$  billion years is the physical time at present epoch or the age of universe. Similarly, the direct cascade of potential energy from large to small scale has a constant rate of  $-1.4\varepsilon_u > 0$ . The total energy of entire self-gravitating collisionless system is decreasing with time as  $E_y = 0.4\varepsilon_u t < 0$  due to the gravitational virialization. With the continuous direct cascade of potential energy down to the smallest scale, a viable mechanism is required to dissipate the cascaded energy on that scale which leads to the decreasing total energy  $E_y$ . For velocity dispersion  $u$  reaching the maximum speed (the speed of light  $c$  in Eq. (4)), the time required is around  $\tau_X = c^2/\varepsilon_u \approx 10^{16} \text{ yrs}$  that might be relevant to the lifetime of dark matter (see Section 6 for more details). Dark matter with a lifetime longer than  $\tau_X$  might have a velocity dispersion exceeding the speed of light.

Other simulations might have a different value of  $u_0$ , but should be on the same order. The constant  $\varepsilon_u$  has a physical meaning as the rate of energy cascade across different scales. The existence of a negative  $\varepsilon_u < 0$  reflects the inverse cascade of kinetic energy from small to large scales (see Fig. 2).

## 3 TWO-THIRDS LAW FROM SIMULATION

Different types of statistical measures are traditionally used to characterize the turbulent flow, i.e. the correlation functions, structure functions, and power spectrum. In this paper, we focus on the structure functions that describe how energy is distributed and transferred across different length scales. In N-body simulations, for a pair of particles at locations  $\mathbf{x}$  and  $\mathbf{x}'$  with velocity  $\mathbf{u}$  and  $\mathbf{u}'$ , the second order longitudinal structure function  $S_2^{lp}$  (pairwise velocity dispersion in cosmology terms) simply reads

$$S_2^{lp}(r, a) = \langle (\Delta u_L)^2 \rangle = \langle (u'_L - u_L)^2 \rangle, \quad (5)$$

where  $u_L = \mathbf{u} \cdot \hat{\mathbf{r}}$  and  $u'_L = \mathbf{u}' \cdot \hat{\mathbf{r}}$  are two longitudinal velocities. The distance  $r \equiv |\mathbf{r}| = |\mathbf{x}' - \mathbf{x}|$  and the unit vector  $\hat{\mathbf{r}} = \mathbf{r}/r$  (see Fig. 3).

For a given scale  $r$ , all particle pairs with the same separation

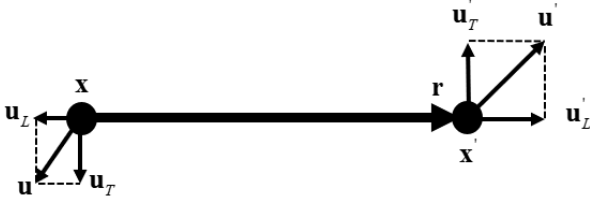


**Figure 3.** Sketch of longitudinal and transverse velocities, where  $\mathbf{u}_T$  and  $\mathbf{u}'_T$  are transverse velocities at two locations  $\mathbf{x}$  and  $\mathbf{x}'$ .  $u_L$  and  $u'_L$  are two longitudinal velocities.

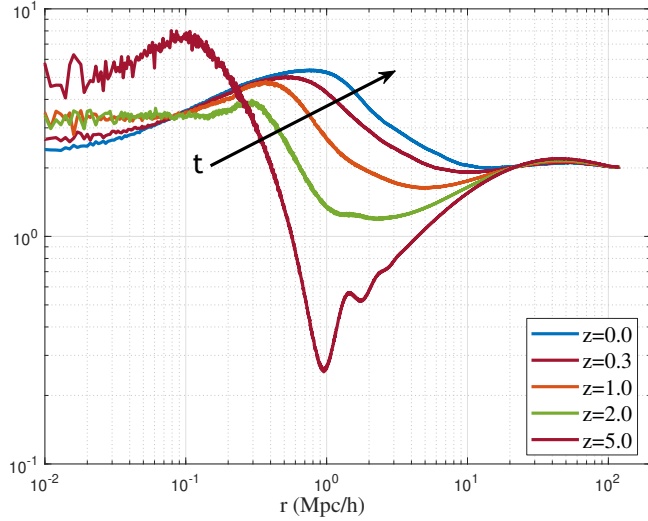


**Figure 4.** The variation of second order longitudinal structure function with scale  $r$  and redshift  $z$ . The structure function  $S_2^{lp}$  (pairwise velocity dispersion) is normalized by velocity dispersion  $u^2(z)$ . Two limits  $\lim_{r \rightarrow 0} S_2^{lp} = \lim_{r \rightarrow \infty} S_2^{lp} = 2u^2$  can be identified on small and large scales.

$r$  can be identified from the simulation. The particle position and velocity data were recorded to compute the structure function in Eq. (5) by averaging that quantity over all particle pairs with the same separation  $r$  (pairwise average). Figure 4 presents the variation of  $S_2^{lp}$  with scale  $r$  at different redshift  $z = 1/a - 1$ , while Figure 5 plots the variation of  $\langle u_L^2 \rangle$  (the variance of  $u_L$ ) with scale  $r$ .

There exist limits  $\lim_{r \rightarrow 0} S_2^{lp} = \lim_{r \rightarrow \infty} S_2^{lp} = 2u^2$  because the correlation coefficient  $\rho_L$  between  $u_L$  and  $u'_L$  has a limit  $\lim_{r \rightarrow 0} \rho_L = 1/2$  on small scale and  $\lim_{r \rightarrow \infty} \rho_L = 0$  on large scale. Therefore, we should have (see Fig. 5)

$$\lim_{r \rightarrow 0} \langle u_L^2 \rangle = \lim_{r \rightarrow 0} \langle u'_L{}^2 \rangle = 2 \lim_{r \rightarrow 0} \langle u_L u'_L \rangle = 2u^2$$

and

$$\lim_{r \rightarrow \infty} \langle u_L^2 \rangle = \lim_{r \rightarrow \infty} \langle u'_L{}^2 \rangle = u^2,$$

where  $\lim_{r \rightarrow 0} \langle u_L u'_L \rangle = \lim_{r \rightarrow 0} \rho_L \langle u_L^2 \rangle = u^2$ . By contrast,  $\langle u_L^2 \rangle = u^2$  on all scales for incompressible hydrodynamic turbulence. Here  $u^2$  is the velocity dispersion of all dark matter particles at redshift  $z$ .

The original scaling law for turbulence postulates that  $S_2^{lp} \propto \varepsilon^{2/3} r^{2/3}$  in the inertial range (Eq. (2)), where the effect of viscosity is negligible in inertial range (Kolmogoroff 1941). Here  $\varepsilon$  is the rate

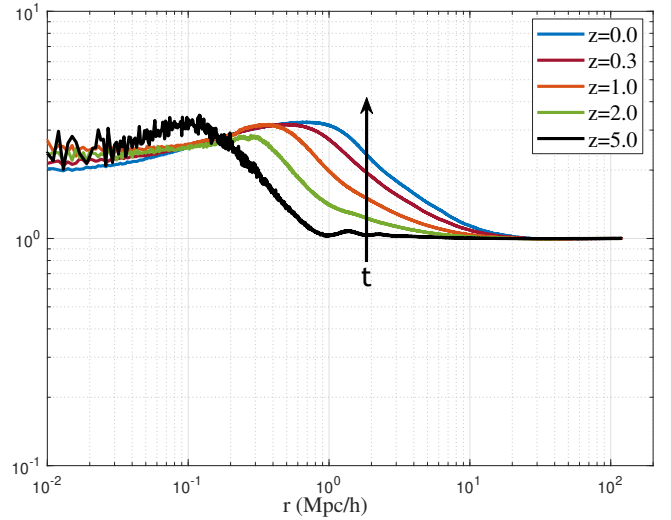


**Figure 5.** The variation of longitudinal velocity dispersion with scale  $r$  and redshift  $z$ . The longitudinal dispersion  $\langle u_L^2 \rangle$  is normalized by velocity dispersion  $u^2(z)$  of entire system. Two limits  $\lim_{r \rightarrow 0} \langle u_L^2 \rangle = 2u^2$  and  $\lim_{r \rightarrow \infty} \langle u_L^2 \rangle = u^2$  can be identified on small and large scales. By contrast,  $\langle u_L^2 \rangle = u^2$  on all scales for incompressible hydrodynamic turbulence.

of direct energy cascade from large to small length scales in Fig. 1. Figure 4 clearly tells us that the original scaling law in turbulence (Eq. (1)) is not valid for dark matter flow due to its collisionless nature. However, a new scaling law can be established for dark matter flow as follows (the two-thirds law in Eq. (7)):

First, halo cores should be incompressible due to the stable clustering hypothesis, i.e. no net stream motion in proper coordinate along halo radial direction such that the proper velocity of dark matter is incompressible on small scales. This prediction hints to a similar scaling law might exist for dark matter flow. Second, just like the incompressible turbulence, energy cascade with a constant rate  $\varepsilon_u$  also exists in dark matter flow, but in an opposite direction. Therefore, it would be reasonable to expect the second order structure function  $S_2^{lp}$  is related to  $\varepsilon_u$  in some way, but different from Eq. (2).

In turbulence, the structure function  $\lim_{r \rightarrow 0} S_2^{lp} = 0$  with  $\lim_{r \rightarrow 0} \rho_L = 1$  because of the viscous force. However, in dark matter flow, the small-scale limit  $\lim_{r \rightarrow 0} S_2^{lp} = 2u^2 \neq 0$  due to the collisionless nature (Fig. 4).

Instead, a reduced structure function  $S_{2r}^{lp} = S_2^{lp} - 2u^2$  can be constructed to restore the same limit  $\lim_{r \rightarrow 0} S_{2r}^{lp} = 0$  as that in turbulence.

This is a simple "renormalization" to deal with the non-vanishing limiting pairwise velocity dispersion at  $r = 0$  in collisionless system.

Pair of particles with a small separation  $r$  is more likely from the same halo (two particles in the same halo), while different pairs can be from different haloes of different size (see Fig. 6). The original pairwise dispersion  $S_2^{lp}$  represents the total kinetic energy of particle pairs on scale  $r$  including the kinetic energy both from the relative motion of particle pairs and from the halo that particle pair resides in. The reduced structure function  $S_{2r}^{lp} = S_2^{lp} - 2u^2$  represents only the kinetic energy  $v_r^2$  from the relative motion of two particles. This description indicates that  $S_{2r}^{lp}$  should be determined by and only by  $\varepsilon_u$  (unit:  $m^2/s^3$ ), scale  $r$ , and gravitational constant  $G$ . By a simple dimensional analysis, the reduced structure function  $S_{2r}^{lp}$  must follow a two-thirds law for small  $r$ , i.e.  $S_{2r}^{lp} \propto v_r^2 \propto (-\varepsilon_u)^{2/3} r^{2/3}$ .



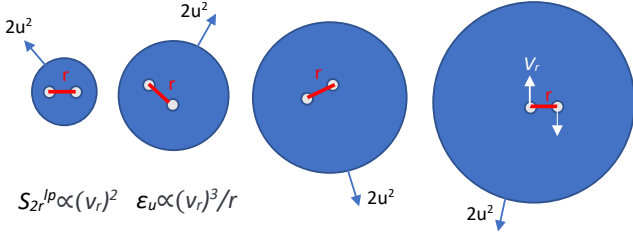


**Figure 6.** On small scale  $r$ , pair of particles is likely from the same halo. Different pairs can be from haloes of different size. The kinetic energy of entire halo ( $2u^2$ ) is relatively independent of halo size. The reduced structure function  $S_{2r}^{lp} = S_2^{lp} - 2u^2$  represents the portion of kinetic energy ( $v_r^2$ ) due to relative motion in particle pair that should be cascaded across scales with a constant rate  $\epsilon_u$ .

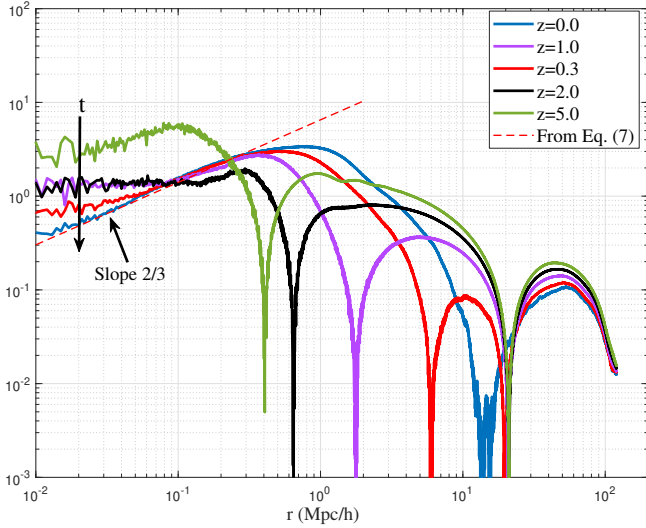


**Figure 7.** The variation of reduced structure function  $S_{2r}^{lp}(r)$  with scale  $r$  and redshift  $z$ . Structure function is normalized by velocity dispersion  $u^2(z)$ . A two-thirds law  $S_{2r}^{lp} \propto (-\epsilon_u)^{2/3} r^{2/3}$  can be identified on small scale below a length scale  $r_l = -u_0^3/\epsilon_u$ , when inverse energy cascade is established with rate  $\epsilon_u$  in Eq. (4). The model from Eq. (7) is also presented for comparison.

Figure 7 plots the variation of reduced structure function  $S_{2r}^{lp}$  with scale  $r$  at different redshifts  $z$  from N-body simulation. The range with  $S_{2r}^{lp} \propto r^{2/3}$  can be clearly identified below a length scale  $r_l = -u_0^3/\epsilon_u$ . This range is formed along with the formation of haloes and the establishment of inverse energy cascade. As expected, the reduced structure function quickly converges to  $S_{2r}^{lp} \propto (-\epsilon_u)^{2/3} r^{2/3}$  with time. The second order reduced longitudinal structure function on small scale now reads (normalized by  $a^{3/2} \propto t$ )

$$S_{2r}^{lp}(r)/a^{3/2} = \beta_2^* (-\epsilon_u)^{2/3} r^{2/3} \propto v_r^2. \quad (7)$$

The length scale  $r_l$  (size of the largest halo in propagation range) is determined by  $u_0$  and  $\epsilon_u$  (see Fig. 10)

$$r_l = -\frac{u_0^3}{\epsilon_u} = \frac{4}{9} \frac{u_0}{H_0} = \frac{2}{3} u_0 t_0 \approx 1.57 \text{ Mpc}/h. \quad (8)$$

The proportional constant  $\beta_2^* \approx 9.5$  can be found from Fig. 7, where the two-thirds law of Eq. (7) is also presented for comparison.

The higher order structure functions can be similarly studied. We can demonstrate that all even order reduced structure functions in Eq. (5) follow the two-thirds law  $\langle (\Delta u_L)^{2n} \rangle \propto r^{2/3}$ , while odd order

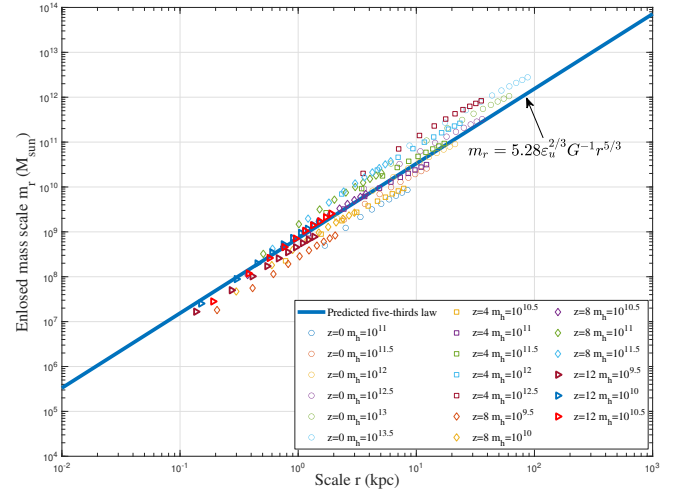


**Figure 8.** The variation of enclosed mass  $m_r$  with scale  $r$  at different redshift from Illustris simulation. For all haloes with a given mass  $m_h$ , the average scale radius  $r_s$  is calculated. The enclosed mass  $m_r$  is computed for different scale  $r$  from  $r = 0.1r_s$  to  $r = r_s$  with an increment of  $0.1r_s$ . Results confirm the predicted five-thirds law in Eq. (10).

structure functions  $\langle (\Delta u_L)^{2n+1} \rangle \propto r$  on small scale (Xu 2022e). Results for high order structure functions are completely different from that of hydrodynamic turbulence in Eq. (1).

#### 4 FIVE-THIRDS AND FOUR-THIRDS LAWS

The two-thirds law on small scale (Eq. (7)) is validated by N-body simulations in Fig. 7, which can be equivalently written as

$$(2v_r^2/r) v_r = 2v_r^2/(r/v_r) = (-\lambda_u \epsilon_u), \quad (9)$$

where  $\lambda_u$  is just a dimensionless numerical constant on the order of unity. Equation (9) describes the cascade of kinetic energy with a constant rate  $\epsilon_u$ . The kinetic energy  $v_r^2$  on scale  $r$  is cascaded to large scale during a turnaround time of  $t_r = r/v_r$ .

Combining Eq. (9) with the virial theorem  $Gm_r/r \propto v_r^2$  on scale  $r$ , we can easily obtain the mass scale  $m_r$  (mass enclosed within  $r$ ), density scale  $\rho_r$  (mean halo density enclosed within  $r$ ), velocity scale  $v_r$  (circular velocity at  $r$ ), and time  $t_r$ , all determined by three quantities  $\epsilon_u$ ,  $G$ , and the scale  $r$ :

$$m_r = \alpha_r \epsilon_u^{2/3} G^{-1} r^{5/3}, \quad \rho_r = \beta_r \epsilon_u^{2/3} G^{-1} r^{-4/3}, \quad (10)$$

$$v_r \propto (-\epsilon_u)^{1/3}, \quad t_r \propto (-\epsilon_u)^{-1/3} r^{2/3},$$

where  $\alpha_r$  and  $\beta_r$  are two numerical constants. To validate the predicted scaling laws, we first presents the results from Illustris simulation (Nelson et al. 2015). Figure 8 plots the variation of enclosed mass scale  $m_r$  with scale  $r$  from Illustris simulation. For all haloes identified with a given mass  $m_h$  at different redshift, the mean scale radius  $r_s$  can be computed, where the logarithmic halo density slope is  $-2$ . For scale  $r$  from  $r = 0.1r_s$  to  $r = r_s$  with an increment of  $0.1r_s$ , we compute the variation of enclosed halo mass  $m_r$  with scale  $r$  and present in Fig. 8. The mass scaling  $m_r \propto r^{5/3}$  is also plotted for comparison with constant  $\alpha_r = 5.28$ . The mass density enclosed within scale  $r$  can be similarly computed. Figure 9 describes the variation of mean halo density  $\rho_r = m_r/(4/3\pi r^3)$  with scale  $r$ . The density scaling  $\rho_r \propto r^{-4/3}$  is also presented for comparison with constant  $\beta_r = 1.26$ . Both figures confirm the predicted scaling laws in Eq. (10).

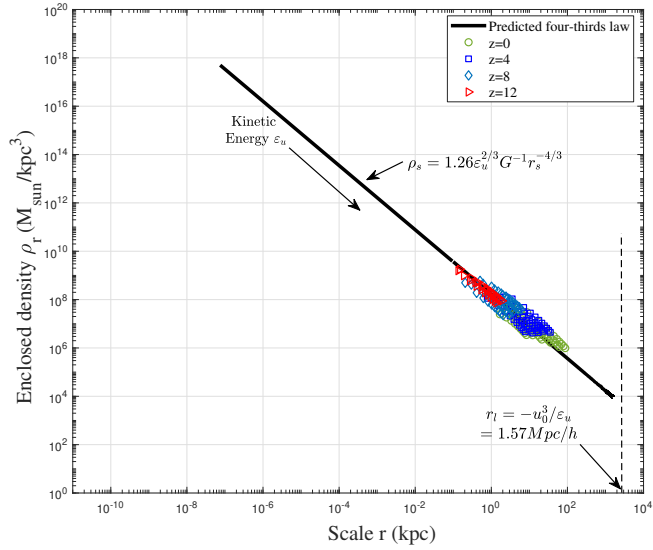


**Figure 9.** The variation of enclosed halo density  $\rho_r$  with scale  $r$  at different redshift from Illustris simulation. The enclosed density  $\rho_r$  is computed from enclosed mass  $m_r$  in Fig. 8 for different scale  $r$ . Results confirm the predicted four-thirds law for halo density in Eq. (10).

Now let us focus on the observational evidence of predicted scaling laws. The four-thirds law  $\rho_r(r) \propto r^{-4/3}$  for mean mass density enclosed within scale  $r$  can also be directly compared against the data from galaxy rotation curves (see Fig. 10). Important information for dark matter haloes can be extracted from galaxy rotation curves by decomposing them into contributions from different mass components. Once the halo density model is selected, the scale radius  $r_s$  and mean density  $\rho_s$  within  $r_s$  can be rigorously obtained by fitting to the decomposed rotation curve. In this work, for pseudo-isothermal (pISO) (Adams et al. 2014) and NFW density models (Navarro et al. 1997), three different sources of galaxy rotation curves are used to extract the halo scale radius  $r_s$  and halo density  $\rho_s$  within  $r_s$ ,

- (i) SPARC (Spitzer Photometry & Accurate Rotation Curves) including 175 late-type galaxies (Lelli et al. 2016; Li et al. 2020);
- (ii) DMS (DiskMass Survey) including 30 spiral galaxies (Martinson et al. 2013);
- (iii) SOFUE (compiled by Sofue) with 43 galaxies (Sofue 2016).

Figure 10 presents the variation of halo core density  $\rho_s$  with scale  $r_s$  obtained from galaxy rotation curves (square and circle symbols). Each symbol represents data from a single galaxy. The four-thirds law (Eq. (10)) is also plotted (thick line) with constants  $\beta_r = 1.26$  or  $\alpha_r = 5.28$  obtained from these data. From this figure, dark matter haloes follow the four-thirds law across six orders.

## 5 COLLISIONLESS DARK MATTER PROPERTIES

Since viscosity is absent in fully collisionless dark matter flow, the scale-independent constant rate of energy cascade  $\varepsilon_u$  in Eq. (4) should extend down to the smallest scale where quantum effects become important. Assuming gravity is the only interaction between unknown dark matter particles (traditionally denoted by  $X$ ), the dominant physical constants on that scale are the (reduced) Planck constant  $\hbar$ , the gravitational constant  $G$ , and the rate of energy cascade  $\varepsilon_u$ . Other physical quantities can be easily found by a simple dimensional

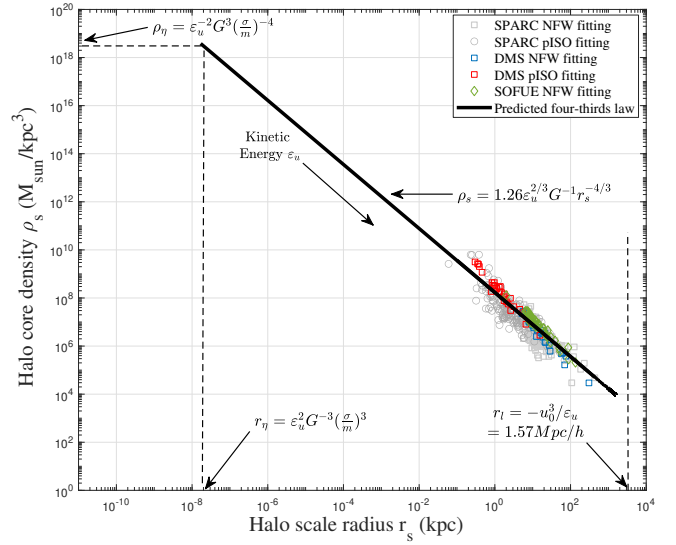


**Figure 10.** The four-thirds law compared against data from galaxy rotation curves. Good agreement confirms the existence of inverse energy cascade with a constant rate  $\varepsilon_u$ . The self-interacting dark matter model with a cross-section  $\sigma/m$  leads to the smallest structure with a size  $r_\eta$  and a maximum density  $\rho_\eta$  determined by  $\varepsilon_u$ ,  $G$ , and  $\sigma/m$  (Table 1), below which no coherent structure can exist. The largest scale  $r_l$  is determined by the velocity dispersion  $u_0$  and  $\varepsilon_u$  (Eq. (8)).

analysis. Two examples are the mass and length scales,

$$m_X = \left( -\varepsilon_u \hbar^5 / G^4 \right)^{\frac{1}{9}} \quad (11)$$

and

$$l_X = (-G\hbar/\varepsilon_u)^{\frac{1}{3}}. \quad (12)$$

The two-thirds law (or the four-thirds law) identified in dark matter flow (Figs. 7 and 9) should also extend down to the smallest length scale if and only if gravity is the only force without any other known interactions. A refined treatment to couple relevant laws on the smallest scale may offer more complete solutions than a simple dimensional analysis. Let's consider two  $X$  particles on the smallest scale with a separation  $r = l_X$  in the rest frame of center of mass,

$$m_X V_X \cdot l_X / 2 = \hbar, \quad (13)$$

$$2V_X^3 / l_X = a_X \cdot v_X = -\lambda_u \varepsilon_u, \quad (14)$$

$$Gm_X / l_X = 2V_X^2, \quad (15)$$

where Eq. (13) is from the uncertainty principle for momentum and position if  $X$  particles exhibit the wave-particle duality. Equation (14) is the "uncertainty" principle for particle acceleration and velocity due to scale-independent energy flux  $\varepsilon_u$ , which is also the two-thirds law in Eq. (9). The last Eq. (15) is from the virial theorem for potential and kinetic energy. Finally, with the following values for three constants

$$\begin{aligned} \varepsilon_u &= -4.6 \times 10^{-7} \text{ m}^2/\text{s}^3, \\ \hbar &= 1.05 \times 10^{-34} \text{ kg} \cdot \text{m}^2/\text{s}, \\ G &= 6.67 \times 10^{-11} \text{ m}^3/(\text{kg} \cdot \text{s}^2), \end{aligned} \quad (16)$$

complete solutions of Eqs. (13)-(15) are (with  $\lambda_u = 1$ )

$$l_X = \left( -\frac{2G\hbar}{\lambda_u \varepsilon_u} \right)^{\frac{1}{3}} = 3.12 \times 10^{-13} m, \quad (17)$$

$$t_X = \frac{l_X}{V_X} = \left( -\frac{32G^2\hbar^2}{\lambda_u^5 \varepsilon_u^5} \right)^{\frac{1}{9}} = 7.51 \times 10^{-7} s,$$

$$m_X = \left( -\frac{256\lambda_u \varepsilon_u \hbar^5}{G^4} \right)^{\frac{1}{9}} = 1.62 \times 10^{-15} kg \approx 10^{12} GeV, \quad (18)$$

$$V_X = \left( \frac{\lambda_u^2 \varepsilon_u^2 \hbar G}{4} \right)^{\frac{1}{9}} = 4.16 \times 10^{-7} m/s, \quad (19)$$

$$a_X = \left( -\frac{4\lambda_u^7 \varepsilon_u^7}{\hbar G} \right)^{\frac{1}{9}} = 1.11 m/s^2.$$

The time scale  $t_X$  is close to the characteristic time for weak interactions ( $10^{-6} \sim 10^{-10} s$ ), while the length scale  $l_X$  is greater than the characteristic range of strong interaction ( $\sim 10^{-15} m$ ) and weak interaction ( $\sim 10^{-18} m$ ). By assuming a scale-independent rate of energy cascade  $\varepsilon_u$  down to the smallest scale, we may obtain all relevant properties for collisionless dark matter particles.

The "thermally averaged cross section" of  $X$  particle is around  $l_X^2 V_X = 4 \times 10^{-32} m^3/s$ . This is on the same order as the cross section required for the correct abundance of today via a thermal production ("WIMP miracle"), where  $\langle \sigma v \rangle \approx 3 \times 10^{-32} m^3 s^{-1}$ . The "cross section  $\sigma/m$ " for  $X$  particle is extremely small, i.e.  $l_X^2/m_X = 6 \times 10^{-11} m^2/kg$ , which means that the dark matter is effectively collisionless.

In addition, a new constant  $\mu_X$  (the scale for the rate of energy dissipation) can be introduced,

$$\mu_X = m_X a_X \cdot V_X = F_X \cdot V_X = -m_X \varepsilon_u$$

$$= \left( -\frac{256\varepsilon_u^{10}\hbar^5}{G^4} \right)^{\frac{1}{9}} = 7.44 \times 10^{-22} kg \cdot m^2/s^3 \quad (20)$$

which is a different representation of  $\varepsilon_u$ . In other words, the fundamental physical constants on the smallest scale can be  $\hbar$ ,  $G$ , and the power constant  $\mu_X$ . An energy scale on that scale is set by

$$E_X = \mu_X t_X / 4 = \hbar / t_X = \sqrt{\hbar \mu_X} / 2 = 0.87 \times 10^{-9} eV. \quad (21)$$

This energy scale is equivalent to a Compton wavelength of 1.4km or a frequency of 0.2MHz. It can be relevant to the possible dark "radiation" and dark matter decay on the smallest scale (see Section 6 for details).

The relevant mass density is around  $m_X / l_X^3 \approx 5.33 \times 10^{22} kg/m^3$ , much larger than the nuclear density that is on the order of  $10^{17} kg/m^3$ . The pressure scale is

$$P_X = \frac{m_X a_X}{l_X^2} = \frac{8\hbar^2}{m_X} \rho_{nX}^{5/3} = 1.84 \times 10^{10} P_a, \quad (22)$$

which sets the highest pressure or the possible "degeneracy" pressure of dark matter that stops further gravitational collapse. Equation (22) is an analogue of the degeneracy pressure of ideal Fermi gas, where  $\rho_{nX} = l_X^{-3}$  is the particle number density. With today's dark matter density around  $2.2 \times 10^{-27} kg/m^3$  and local density  $7.2 \times 10^{-22} kg/m^3$ , the mean separation between  $X$  particles is about  $l_u \approx 10^4 m$  in the entire universe and  $l_c \approx 130 m$  locally.

The predicted mass scale is around  $0.9 \times 10^{12} GeV$  (Eq. (18)).

This is well beyond the mass range of standard thermal WIMPs, but in the range of nonthermal relics, the so-called super heavy dark matter (SHDM). Our prediction is not dependent on the production mechanism of dark matter. One example mechanism can be the gravitational particle production in quintessential inflation (Ford 1987; Haro & Saló 2019). The nonthermal relics from gravitational production do not have to be in the local equilibrium in early universe or obey the unitarity bounds for thermal WIMPs. To have the right abundance generated during inflation, these nonthermal relics should also have a mass range between  $10^{12}$  and  $10^{13} GeV$  (Chung et al. 1999; Kolb & Long 2017). The other possible super-heavy dark matter candidate is the crypton in string or M theory with a mass around  $10^{12} GeV$  to give the right abundance (Ellis et al. 1990; Benakli et al. 1999). Our prediction of dark matter particle properties should provide more insights on the possible production mechanism. Potential direct and indirect detection methods for ultra-heavy dark matter were also discussed (Carney et al. 2022; Blanco et al. 2022).

To have the right abundance of dark matter at the present epoch, SHDM must be stable with a lifetime much greater than the age of universe. In the first scenario, if  $X$  particles directly decay or annihilate into standard model particles, the products could be detected indirectly. The decay of SHDM particles could be the source of ultra-high energy cosmic rays (UHECR) above the Greisen-Zatsepin-Kuzmin cut-off (Greisen 1966). Constraints on the mass and lifetime of SHDM can be obtained from the absence of ultra-high-energy photons and cosmic ray (Anchordoqui et al. 2021). For a given mass scale of  $10^{12} GeV$ , the lifetime is expected to be  $\tau_X \geq 5 \times 10^{22} yr$ . In addition, if instantons are responsible for the decay, lifetime can be estimated by (Anchordoqui et al. 2021)

$$\tau_X \approx \frac{\hbar e^{1/\alpha_X}}{m_X c^2}, \quad (23)$$

where  $\alpha_X$  is a coupling constant on the scale of the interaction considered. With the lifetime  $\tau_X \geq 5 \times 10^{22} yr$ , the coupling constant should satisfy  $\alpha_X \leq 1/152.8$  from Eq. (23).

For comparison, a different (second) scenario can be proposed. There can be a slow decay for  $X$  particle with an energy on the order of  $E_X$  in Eq. (21). In this slow decay scenario, the lifetime it takes for a complete decay of a single  $X$  particle can be estimated as,

$$\tau_X = \frac{m_X c^2}{\mu_X} = -\frac{c^2}{\varepsilon_u} \approx \frac{\hbar e^{1/\alpha_X}}{m_X c^2}, \quad (24)$$

where the lifetime  $\tau_X \approx 2 \times 10^{23} s = 6.2 \times 10^{15} yrs$  is also much greater than the age of our universe, but shorter than the lifetime in the first scenario. The coupling constant of this scenario is estimated as  $\alpha_X \approx 1/136.85$  from Eq. (24). Since  $\varepsilon_u$  is the proportional constant of kinetic energy  $K_p$  in Eq. (4), Eq. (24) gives the maximum dark matter particle lifetime, beyond which the velocity dispersion  $u$  will exceed the speed of light, which seems implausible.

## 6 AXION DARK "RADIATION" AND ITS PROPERTIES

The energy scale  $E_X \approx (\varepsilon_u^5 \hbar^7 G^{-2})^{1/9} = 10^{-9} eV$  in Eq. (21) strongly suggests the existence of a dark "radiation" field that is coupled to the predicted dark matter particles of mass around  $10^{12} GeV$ . Similar to the phonon radiation in superfluid turbulence to dissipate the system kinetic energy, the dark "radiation" associated with the collisionless dark matter provides a viable mechanism to dissipate the total energy cascaded to the smallest scale  $l_X$ . Though the nature of this dark "radiation" particle is still not clear, it should be produced around the time  $t_X \approx 10^{-6} s$  (during quark epoch) with a mass on the order

of the energy scale  $E_X \sim 10^{-9}\text{eV}$  to satisfy the uncertainty principle  $t_X E_X \approx \hbar$ . These properties hint that axion particle can be a very promising candidate due to its small mass and weak interaction with standard model (SM) particles (Mazumdar et al. 2016; Marsh 2016). In this section, we will take axion as the dark "radiation" and predict its potential properties and constraints.

If axion is the dark "radiation" responsible for the energy dissipation, it should have a mass on the order of  $m_a \sim E_X = 10^{-9}\text{eV}$ . Since axion mass is closely related to the decay constant  $f_a$  according to equation (Chadha-Day et al. 2022),

$$m_a = (5.70 \pm 0.007) \times 10^{-6}\text{eV} \left( \frac{10^{12}\text{GeV}}{f_a} \right). \quad (25)$$

This leads to a GUT (grand unification energy) energy scale at which the Peccei-Quinn (PQ) symmetry is spontaneously broken, i.e.  $f_a \approx 6.5 \times 10^{15}\text{GeV}$ . Axion particle with these properties should obtain its mass at a critical temperature of  $T_1 \approx 230\text{ MeV}$  during the quark epoch. QCD axion's coupling to SM particles is inversely proportional to  $f_a$ , which leads to an extremely weak coupling to photons with an effective coupling constant  $g_{a\gamma\gamma} \sim 10^{-18}\text{GeV}^{-1}$ . This is beyond the range of current direct search of axion (Semertzidis & Youn 2022), but should be covered within the next decade.

The energy density of dark "radiation" should be related to  $\rho_{\text{DM}}\epsilon_u t_0$ , where  $\rho_{\text{DM}}$  is today's dark matter density. The abundance of dark "radiation" can be estimated as

$$\frac{\Omega_a h^2}{\Omega_{\text{DM}} h^2} = \frac{\epsilon_u t_0}{c^2} = 2.2 \times 10^{-6}, \quad (26)$$

where  $\Omega_{\text{DM}} h^2 = 0.119$  is the dark matter density parameter (Planck Collaboration et al. 2014). From this, the dark radiation should have a density of  $\Omega_a h^2 \approx 2.6 \times 10^{-7}$ , which is about 1 percent of the photon energy in CMB ( $\Omega_\gamma h^2 \approx 2.5 \times 10^{-5}$ ). The abundance of relativistic dark radiation can also be parameterized by the increase in the effective number of neutrino species (Higaki et al. 2013). Based on our estimation, this increase at present epoch is given by

$$\Delta N_{\text{eff}} = \frac{8}{7} \left( \frac{11}{4} \right)^{1/3} \frac{\Omega_a h^2}{\Omega_\gamma h^2} \approx 0.02. \quad (27)$$

The dark radiation was proposed to alleviate the disagreements of the current expansion rate  $H_0$  and the amplitude of matter fluctuation  $S_8$  between  $\Lambda\text{CDM}$  model prediction and the direct measurement in the local universe, namely the Hubble tension and  $S_8$  tension (Pandey et al. 2020; Chen et al. 2021). With dark matter and axion dark "radiation" properties presented in this work, more study is required for their effects on the cosmological observations and disagreements.

## 7 SELF-INTERACTING DARK MATTER

Note that the mass scale  $m_X$  is only weakly dependent on  $\epsilon_u$  as  $m_X \propto \epsilon_u^{1/9}$  (Eq. (18)) such that the estimation of  $m_X$  should be pretty robust for a wide range of possible values of  $\epsilon_u$ . A small change in  $m_X$  requires huge change in  $\epsilon_u$ . Unless gravity is not the only interaction, the uncertainty in predicted  $m_X$  should be small. In other words, if our estimation of  $\epsilon_u$  (Eq. (4)) is accurate and gravity is the only interaction on the smallest scale, it seems not possible for dark matter particle with any mass far below or above  $10^{12}\text{GeV}$  to produce the given value of energy cascade rate  $\epsilon_u \approx 10^{-7}m^2/s^3$ . If mass has a different value, there must be some new interaction beyond gravity. This can be the self-interacting dark matter (SIDM) model as a potential solution for "cusp-core" problem (Spergel & Steinhardt 2000).

**Table 1.** Physical scales for the flow of dark matter

Scales	Fully collisionless	Self-interacting
Length	$l_X = (-2G\hbar/\epsilon_u)^{1/3}$	$r_\eta = \epsilon_u^2 G^{-3} (\sigma/m)^3$
Time	$t_X = (-32G^2\hbar^2/\epsilon_u^5)^{1/9}$	$t_\eta = \epsilon_u G^{-2} (\sigma/m)^2$
Mass	$m_X = (-256\epsilon_u\hbar^5/G^4)^{1/9}$	$m_\eta = \epsilon_u^4 G^{-6} (\sigma/m)^5$
Density	$\rho_X = (\epsilon_u^{10}\hbar^{-4}/G^{13})^{1/9}$	$\rho_\eta = \epsilon_u^{-2} G^3 (\sigma/m)^{-4}$

For self-interacting dark matter, a key parameter is the cross section  $\sigma/m$  (in unit:  $m^2/kg$ ) of self-interaction that can be constrained by various astrophysical observations. Self-interaction introduces an additional scale, below which the self-interaction is dominant over gravity to suppress all small-scale structures and the two-thirds law is no longer valid. In this case, the dark matter particle properties can be obtained only if the nature and dominant constants of self-interaction is known. The lowest scale for two-thirds law is related to three constants in principle, i.e. the rate of energy cascade  $\epsilon_u$ , the gravitational constant  $G$ , and the cross section  $\sigma/m$ . In other words, the cross section might be estimated if the scale of the smallest structure is known. Taking the value of  $\sigma/m = 0.01m^2/kg$  used for cosmological SIDM simulation to reproduce the right halo core size and central density (Rocha et al. 2013), Table 1 lists the relevant quantities on the smallest scale for both collisionless and self-interacting dark matter (also plotted in Fig. 10). More insights can be obtained by extending the current statistical analysis to self-interacting dark matter simulations.

## 8 CONCLUSIONS

A cascade theory is proposed for dark matter flow to identify properties of dark matter particles. The dark "radiation" is proposed to be responsible for the energy dissipation. The energy cascade leads to a two-thirds law for pairwise velocity, or equivalently five-thirds and four-thirds laws for halo mass and halo density. All scaling laws can be confirmed by cosmological N-body simulations and galaxy rotation curves. For collisionless dark matter, viscosity is not present and gravity is the only interaction such that the established scaling laws can be extended to the smallest scale, where quantum effects become important. The dominant constants on that scale include the constant rate of energy cascade  $\epsilon_u$ , Planck constant  $\hbar$ , and gravitational constant  $G$ . Dark matter particles are found to have a mass  $m_X = (\epsilon_u\hbar^5G^{-4})^{1/9} = 0.9 \times 10^{12}\text{GeV}$ , a size  $l_X = (\epsilon_u^{-1}\hbar G)^{1/3} = 3 \times 10^{-13}\text{m}$ , and a lifetime  $\tau_X = c^2/\epsilon_u = 10^{16}\text{yrs}$ , along with other important properties. Potential extension to self-interacting dark matter is also discussed with relevant scales estimated for a given cross section  $\sigma/m$  (see Table 1). The energy scale  $E_X = (\epsilon_u^5\hbar^7G^{-2})^{1/9} = 10^{-9}\text{eV}$  suggests a dark "radiation" field responsible for energy dissipation. If axion is the dark "radiation", it should have a mass  $10^{-9}\text{eV}$  with a GUT scale decay constant  $10^{16}\text{GeV}$  and an effective axion-photon coupling constant  $10^{-18}\text{GeV}^{-1}$ . This work suggests a heavy dark matter scenario with a mass much greater than WIMPs and a dark "radiation" field from dark matter decay.

## DATA AVAILABILITY

Two datasets for this article, i.e. a halo-based and correlation-based statistics of dark matter flow, are available on Zenodo (Xu 2022a,b), along with the accompanying presentation "A comparative study of



dark matter flow & hydrodynamic turbulence and its applications" (Xu 2022c). All data are also available on GitHub (Xu 2022d).

## REFERENCES

- Adams J. J., et al., 2014, *ApJ*, **789**, 63
- Aghanim N., et al., 2021, *Astronomy & Astrophysics*, 652
- Anchordoqui L. A., et al., 2021, *Astroparticle Physics*, 132
- Batchelor G. K., 1953, *The Theory of Homogeneous Turbulence*. Cambridge University Press, Cambridge, UK
- Benakli K., Ellis J., Nanopoulos D. V., 1999, *Phys. Rev. D*, **59**, 047301
- Blanco C., Elshimy B., Lang R. F., Orlando R., 2022, *Physical Review D*, 105
- Boylan-Kolchin M., Bullock J. S., Kaplinghat M., 2011, *Monthly Notices of the Royal Astronomical Society: Letters*, 415, L40
- Boylan-Kolchin M., Bullock J. S., Kaplinghat M., 2012, *Monthly Notices of the Royal Astronomical Society*, 422, 1203
- Bullock J. S., Boylan-Kolchin M., 2017, *ARA&A*, **55**, 343
- Carney D., et al., 2022, Snowmass2021 Cosmic Frontier White Paper: Ultra-heavy particle dark matter, doi:10.48550/ARXIV.2203.06508, <https://arxiv.org/abs/2203.06508>
- Chadha-Day F., Ellis J., Marsh D. J. E., 2022, *Science Advances*, 8, eabj3618
- Chen A., et al., 2021, *Phys. Rev. D*, 103, 123528
- Chung D. J. H., Kolb E. W., Riotto A., 1999, *Physical Review D*, 59
- Colberg J. M., White S. D. M., Jenkins A., Pearce F. R., 1999, *Monthly Notices of the Royal Astronomical Society*, 308, 593
- Cooray A., Sheth R., 2002, *Physics Reports-Review Section of Physics Letters*, 372, 1
- Duffy L. D., van Bibber K., 2009, *New Journal of Physics*, 11, 105008
- Ellis J., Lopez J. L., Nanopoulos D. V., 1990, *Physics Letters B*, 247, 257
- Flores R. A., Primack J. R., 1994, *ApJ*, **427**, L1
- Ford L. H., 1987, *Phys. Rev. D*, 35, 2955
- Frenk C. S., White S. D. M., 2012, *Annalen der Physik*, **524**, 507
- Frenk C. S., et al., 2000, *arXiv:astro-ph/0007362v1*
- Greisen K., 1966, *Phys. Rev. Lett.*, 16, 748
- Griest K., Kamionkowski M., 1990, *Physical Review Letters*, 64, 615
- Haro J., Saló L. A., 2019, *Phys. Rev. D*, 100, 043519
- Higaki T., Nakayama K., Takahashi F., 2013, *Journal of Cosmology and Astroparticle Physics*, 2013, 030
- Irvine W. M., 1961, Thesis, HARVARD UNIVERSITY
- Jenkins A., et al., 1998, *Astrophysical Journal*, 499, 20
- Jungman G., Kamionkowski M., Griest K., 1996, *Physics Reports-Review Section of Physics Letters*, 267, 195
- Klypin A., Kravtsov A. V., Valenzuela O., Prada F., 1999, *The Astrophysical Journal*, 522, 82
- Kolb E. W., Long A. J., 2017, *Physical Review D*, 96
- Kolmogoroff A. N., 1941, *Comptes Rendus De L Academie Des Sciences De L Urss*, 32, 16
- Kolmogorov A. N., 1962, *Journal of Fluid Mechanics*, 13, 82
- Komatsu E., et al., 2011, *ApJS*, **192**, 18
- Kraichnan R. H., 1967, *Physics of Fluids*, 10, 1417
- Layzer D., 1963, *Astrophysical Journal*, 138, 174
- Lelli F., McGaugh S. S., Schombert J. M., 2016, *AJ*, **152**, 157
- Li P., Lelli F., McGaugh S., Schombert J., 2020, *ApJS*, **247**, 31
- Marsh D. J. E., 2016, *Phys. Rep.*, **643**, 1
- Martinsson T. P. K., Verheijen M. A. W., Westfall K. B., Bershadsky M. A., Andersen D. R., Swaters R. A., 2013, *A&A*, **557**, A131
- Mazumdar A., Qutub S., Saikawa K., 2016, *Phys. Rev. D*, 94, 065030
- Mo H., van den Bosch F., White S., 2010, *Galaxy formation and evolution*. Cambridge University Press, Cambridge
- Moore B., Ghigna S., Governato F., Lake G., Quinn T., Stadel J., Tozzi P., 1999, *The Astrophysical Journal*, 524, L19
- Navarro J. F., Frenk C. S., White S. D. M., 1997, *Astrophysical Journal*, 490, 493
- Nelson D., et al., 2015, *Astronomy and Computing*, 13, 12
- Neyman J., Scott E. L., 1952, *Astrophysical Journal*, 116, 144
- Pandey K. L., Karwal T., Das S., 2020, *Journal of Cosmology and Astroparticle Physics*, 2020, 026
- Peebles P. J. E., 1980, *The Large-Scale Structure of the Universe*. Princeton University Press, Princeton, NJ
- Peebles P. J. E., 1984, *ApJ*, **284**, 439
- Perivolaropoulos L., Skara F., 2022, *New Astronomy Reviews*, 95, 101659
- Planck Collaboration et al., 2014, *A&A*, **571**, A16
- Richardson L. F., 1922, *Weather Prediction by Numerical Process*. Cambridge University Press, Cambridge, UK
- Rocha M., Peter A. H. G., Bullock J. S., Kaplinghat M., Garrison-Kimmel S., Oñorbe J., Moustakas L. A., 2013, *Monthly Notices of the Royal Astronomical Society*, 430, 81
- Rubin V. C., Ford W. K., 1970, *Astrophysical Journal*, 159, 379
- Rubin V. C., Ford W. K., Thonnard N., 1980, *Astrophysical Journal*, 238, 471
- Semertzidis Y. K., Youn S., 2022, *Science Advances*, 8, eabm9928
- Sheth R. K., Mo H. J., Tormen G., 2001, *Monthly Notices of the Royal Astronomical Society*, 323, 1
- Sofue Y., 2016, *Publications of the Astronomical Society of Japan*, 68
- Spergel D. N., Steinhardt P. J., 2000, *Phys. Rev. Lett.*, 84, 3760
- Spergel D. N., et al., 2003, *ApJS*, **148**, 175
- Steigman G., Turner M. S., 1985, *Nuclear Physics B*, 253, 375
- Taylor G. I., 1935, *Proceedings of the royal society A*, 151, 421
- Taylor G. I., 1938, *Proceedings of the Royal Society of London Series a-Mathematical and Physical Sciences*, 164, 0015
- Tulin S., Yu H.-B., 2018, *Physics Reports*, 730, 1
- Viel M., Becker G. D., Bolton J. S., Haehnelt M. G., 2013, *Phys. Rev. D*, 88, 043502
- Xu Z., 2022c, A comparative study of dark matter flow & hydrodynamic turbulence and its applications, doi:10.5281/zenodo.6569901, <http://dx.doi.org/10.5281/zenodo.6569901>
- Xu Z., 2022d, Dark matter flow dataset, doi:10.5281/zenodo.6586212, [https://github.com/ZhijieXu2022/dark\\_matter\\_flow\\_dataset](https://github.com/ZhijieXu2022/dark_matter_flow_dataset)
- Xu Z., 2022a, Dark matter flow dataset Part I: Halo-based statistics from cosmological N-body simulation, doi:10.5281/zenodo.6541230, <http://dx.doi.org/10.5281/zenodo.6541230>
- Xu Z., 2022b, Dark matter flow dataset Part II: Correlation-based statistics from cosmological N-body simulation, doi:10.5281/zenodo.6569898, <http://dx.doi.org/10.5281/zenodo.6569898>
- Xu Z., 2022e, *arXiv e-prints*, p. arXiv:2202.06515
- de Blok W. J. G., 2010, *Adv. Astron.*, 2010, 789293
- de Karman T., Howarth L., 1938, *Proceedings of the Royal Society of London Series a-Mathematical and Physical Sciences*, 164, 0192